Kinetics of Heterogeneous Reactions of HO_2 Radical at Ambient Concentration Levels with $(NH_4)_2SO_4$ and NaCl Aerosol Particles

Fumikazu Taketani,* Yugo Kanaya, and Hajime Akimoto

Frontier Research Center for Global Change, Japan Agency for Marine-Earth Science and Technology, 3173-25 Showa-machi, Kanazawa-ku, Yokohoma, Kanagawa 236-0001, Japan

Received: August 31, 2007; In Final Form: December 26, 2007

The HO_2 uptake coefficient (γ) for inorganic submicrometer wet and dry aerosol particles ($(NH_4)_2SO_4$ and NaCl) under ambient conditions (760 Torr and 296 ± 2 K) was measured using an aerosol flow tube (AFT) coupled with a chemical conversion/laser-induced fluorescence (CC/LIF) technique. The CC/LIF technique enabled experiments to be performed at almost the same HO_2 radical concentration as that in the atmosphere. HO_2 radicals were injected into the AFT through a vertically movable Pyrex tube. Injector position-dependent profiles of LIF intensity were measured as a function of aerosol concentration. Measured γ values for dry aerosols of $(NH_4)_2SO_4$ were 0.04 ± 0.02 and 0.05 ± 0.02 at 20% and 45% relative humidity (RH), respectively, while those of NaCl were <0.01 and 0.02 ± 0.01 at 20% and 53% RH, respectively. For wet $(NH_4)_2SO_4$ aerosols, measured γ values were 0.11 ± 0.03, 0.15 ± 0.03, 0.17 ± 0.04, and 0.19 ± 0.04, at 45%, 55%, 65%, and 75% RH, respectively, whereas for wet NaCl aerosols the values were 0.11 ± 0.03, 0.09 ± 0.02, and 0.10 ± 0.02 for 53%, 63%, and 75% RH, respectively. Wet $(NH_4)_2SO_4$ and NaCl aerosols doped with $CuSO_4$ showed γ values of 0.53 ± 0.12 and 0.65 ± 0.17, respectively. These results suggest that compositions, RH, and phase for aerosol particles are significant to HO_2 uptake. Potential HO_2 loss processes and their atmospheric contributions are discussed.

1. Introduction

The hydroxyl (OH) and hydroperoxyl (HO_2) radicals, collectively referred to as HO_x radicals, play central roles in tropospheric chemistry.[1] The concentration levels of OH and HO_2 in the troposphere are close to the steady-state values at which their production and loss rates are balanced. As for the production terms, the photolysis of ozone (followed by the $O(^1D) + H_2O$ reaction) and the $HO_2 + NO$ reaction are important for OH, while the photolysis of HCHO, the OH + CO reaction, and the $RO_2 + NO$ reactions are important for HO_2. The loss of OH is mainly due to reactions with CO, hydrocarbons, and NO_2, while the loss of HO_2 is dominated by reactions with NO, O_3, itself (HO_2), and RO_2.

A number of recent field observations of the HO_x radical, however, revealed that the daytime HO_2 levels estimated from the balance between the known source and sink reactions in the gas phase under the steady-state approximation were higher than observed levels,[2−6] implying that loss processes of HO_2 were missing. Heterogeneous losses of HO_2 on the surface of aerosol particles would be one of the possible processes to explain the difference. Using the uptake coefficient (γ) for HO_2 in the range of 0.1−1, better agreement between the observed and calculated HO_2 levels was achieved in these field studies.[2,3,5]

Heterogeneous reactions of the HO_2 radical have been investigated by several laboratory studies. Remorov et al.[7] studied the loss of HO_2 on solid NaCl using a coaxial reactor with a NaCl coating coupled to an electron paramagnetic resonance (EPR) or an electron spin resonance (ESR). Gershenzon et al.[8] studied the loss of HO_2 by solid inorganic compounds using a cylinder reactor coupled to EPR. These two studies, performed at 1−3 Torr, indicated that the uptake coefficient of HO_2 on solid NaCl is about 0.01 at room temperature. In contrast to the cases using coated surfaces, studies using sub-micrometer aerosol particles for the reaction are rare. Mozurkewich et al.[9] reported the first experiment of heterogeneous loss of HO_2 by wet particles of $(NH_4)HSO_4$ and $LiNO_3$ using a flow tube reactor coupled to a chemical amplifier-luminol detector. Their experiment was performed at $[HO_2] \sim 10^8-10^9$ molecules cm^{-3} and 75% RH. They reported that the mass accommodation coefficients (α) of HO_2 on the $(NH_4)HSO_4$ and $LiNO_3$ wet particles were greater than 0.2 by doping with $CuSO_4$. Their results suggest that the reaction of HO_2 with Cu(II) may play a significant role in scavenging HO_2 when aerosols contain a sufficient amount of Cu(II) ions. Thornton and Abbatt[10] reported measurements of the heterogeneous loss of HO_2 on the H_2SO_4 and $(NH_4)_2SO_4$ wet particles at room temperature using an aerosol flow tube coupled to a chemical ionization mass spectrometer. The initial concentration of HO_2 in their experiment was $\sim 5 \times 10^{10}$ molecules cm^{-3} at 42% RH. Under this condition, the self-reaction of HO_2 in the gas phase cannot be neglected. Their results suggested that the uptake coefficient on the H_2SO_4 particles was <0.01. On $(NH_4)_2SO_4$ particles, γ was estimated to be ~0.1 from the first-order analysis of data at ~42% RH. However, they reported the HO_2 loss was attributed to the self-reaction of HO_2 in the aqueous phase, and thereby they concluded that the uptake coefficient could be <0.01 under the tropospheric condition ($[HO_2] \sim 1 \times 10^8$ molecules cm^{-3}) by extrapolation, although no experiments under tropospheric conditions were performed.

Morita et al.[11] reported that the mass accommodation of the HO_2 radical on the water surface is almost unity using molecular dynamics (MD) computer simulations. Their box model calculations showed that the daytime HO_2 concentration is significantly

* Corresponding author. Fax: +81-45-778-5496. E-mail: taketani@jamstec.go.jp.

10.1021/jp0769936 CCC: $40.75
Published on Web 02/21/2008

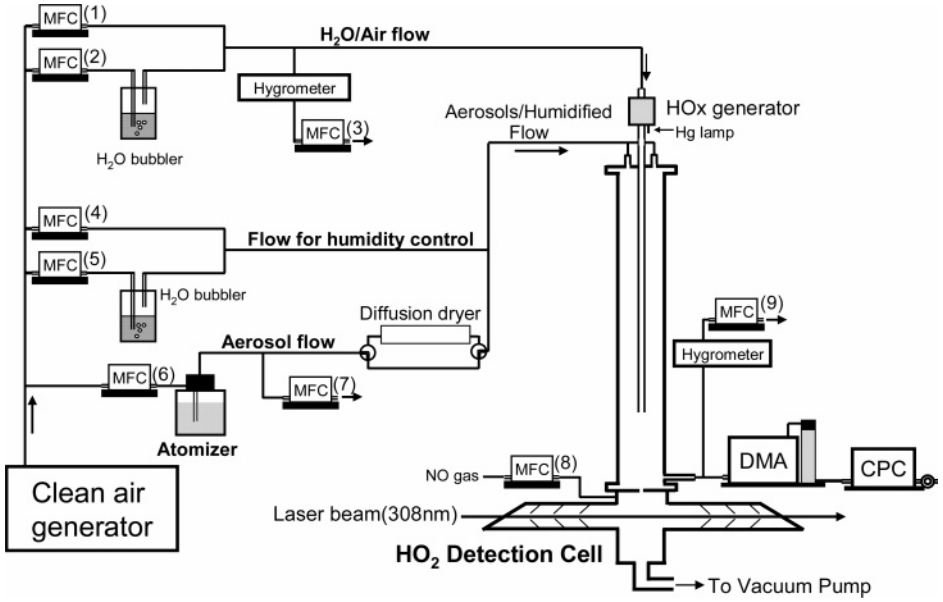

Figure 1. Schematic diagram of the experimental apparatus for measurement of kinetics of HO_2 with aerosols using an aerosol flow tube coupled with a laser-induced fluorescence (LIF) technique. Details are descried in the text. MFC, mass flow controller; DMA, differential mobility analyzer; CPC, condensation particle counter.

sensitive to the assumed uptake coefficient in the range of 0.2−1 under clean marine and urban conditions. Using $\gamma = 0.2$ for any types of aerosol particles in a global tropospheric modeling, Martin et al.[12] showed that the contribution from the heterogeneous loss to the total HO_x loss rate exceeded 80% at the surface level with high aerosol loadings and was about 20% over the Antarctic Ocean. These results suggest that the heterogeneous reaction of HO_2 is potentially important in a geographically wide area. However, more precise evaluation has not been achieved, due to the lack of knowledge for the dependence of γ on the composition and surface conditions of the aerosol particles.

These results suggest that more measurements of the uptake coefficient of HO_2 are needed for various aerosol particle types with different compositions and surface conditions to clarify the importance of the heterogeneous process of HO_2. In the present Article, we report the heterogeneous loss of HO_2 by wet and dry aerosol particles of $(NH_4)_2SO_4$ and NaCl at 296 ± 2 K using an aerosol flow tube (AFT) coupled with chemical conversion/laser-induced fluorescence (CC/LIF). The AFT/CC/LIF technique was applied to the measurement of HO_2 uptake on aerosol particles for the first time. In this study, the $(NH_4)_2SO_4$ and NaCl particles are regarded as typical chemical species in the urban and marine atmosphere, respectively. Because of the high sensitivity of the CC/LIF instrument to HO_2, we are able to measure the HO_2 decays with initial concentrations of $\sim 1 \times 10^8$ molecules cm^{-3}, which are similar to the ambient concentration levels. Furthermore, the effect of the self-reaction of HO_2 in the gas phase can be neglected in the system.

2. Experimental Section

Figure 1shows the schematic experimental setup (AFT/CC/LIF) to study heterogeneous loss of HO_2 by $(NH_4)_2SO_4$ and NaCl aerosols. The kinetics of HO_2 loss in the AFT were measured by changing the position of the HO_2 radical injector to vary the contact time between the HO_2 radical and the aerosol. The change in HO_2 signal was monitored using the LIF technique. All experiments were performed at atmospheric pressure and 296 ± 2 K. The details of the experimental setup are described in the following sections.

2.1. Flow System. All gases were supplied by zero air, and flow rates were regulated by eight mass flow controllers (MFCs) (models 3660 and 3650, Kofloc). The zero air is generated by a zero air generator (Thermo model 111), equipped with a heated Pt catalysist and purafil (alumina impregnated with $KMnO_4$) and charcoal traps. The RH was controlled by mixing a dry airflow with a flow of air passed through a water bubbler. The total volumetric flow rate in the AFT was kept at 10.4 L min^{-1}.

2.2. HO_2 Generation. The HO_2 radical was generated by the photolysis of H_2O using a mercury lamp through a quartz tube (ϕ(O.D.) 6 mm) via the following reactions in 760 Torr air.

$$H_2O + h\nu(185\ nm) \rightarrow OH + H \quad (1)$$

$$H + O_2 + M(N_2\ or\ O_2) \rightarrow HO_2 + M \quad (2)$$

The flow rate including the HO_2 radical was controlled at 0.47 L min^{-1} using MFCs (1, 2, and 3), and H_2O concentration was monitored by a commercial hygrometer. After radical generation, radicals were carried to the AFT through a 100 cm (ϕ(O.D.) 12 mm) Pyrex tube coated with halocarbon wax to avoid wall loss of the HO_2 radical.

2.3. Aerosol Generation. An atomizer (model 3076, TSI) was utilized to generate polydisperse distributions of $(NH_4)_2SO_4$ or NaCl aerosol particles from 0.02 to 0.05 M aqueous solutions. In the case of the measurement of mass accommodation (α) of wet aerosol, $CuSO_4 \cdot 5H_2O$ was added to the aqueous solution as a catalyst[9,10] at a molar ratio of ~5% to $(NH_4)_2SO_4$ or NaCl solutions. When chemical reactions in the interface and/or aqueous phase are rapid, the uptake rate is controlled by accommodation, and the measured value of γ will correspond to α under these conditions. Details are given in section 3.3.

The volumetric flow rate from the atomizer output was adjusted to be 2.9 L min^{-1} using MFC (6). Because the RH just after atomizer output is close to 100%, wet particles can be prepared by regulating RH after the particles are produced by the atomizer. When the RH decreases to below the deliquescence RH (~75%), the droplets do not immediately

effloresce, but remain supersaturated until reaching efflorescence RH (~40%). To generate dry particles, the atomizer output flow was passed through a diffusion dryer (model 3062, TSI) before mixing with the humidified air flow. After that, particles should be dry, because the RH was <20%, below the efflorescence point of ~40% RH.[13] Once the particles are dried, they stay on the solid phase up to a deliquescence RH ~75% due to hysteresis.[13] In the present study, the aerosol particles produced using the dryer are referred to as the "dry particles", and those produced without the dryer are referred to as the "wet particles". Under the same volumetric flow rate (9.9 L min^{-1}), the RH and aerosol concentration were controlled by adjusting the ratios of the humidity-controlled flow to the aerosol flow using MFCs (4, 5, and 7).

All reagents (Kanto Kagaku, purity >99.5%) were used without further purification.

2.4. Aerosol Flow Tube. The AFT (100 cm in height and 6 cm inner diameter) was mounted on the HO_2 detection instrument (LIF cell). The bottom of the AFT faced the inlet pinhole of the LIF instrument. Humidified aerosol flow was introduced from the top of the AFT, and HO_2 radical flow was injected at the center of the AFT using a vertically movable Pyrex tube. The inside of the AFT was coated with halocarbon wax to avoid HO_2 losses by the wall. The RH in the AFT was monitored by a commercial hygrometer, and the RHs before and after the AFT were almost the same within 0.5% in this study. The two flow velocities (in the aerosol and radical flow tubes) were controlled to be close to one another, such that radial mixing between the flows containing radicals and aerosols occurs efficiently. The LIF cell and the aerosol-sizing instrument require a volumetric flow rate of ~9 and 0.6 L min^{-1}, respectively. In our experimental conditions, the linear flow velocity was 6.1 cm s^{-1} and Reynolds number was ~250, suggesting that the flow condition in the AFT was laminar.

The mixing time of the two flows is given by $r^2/5D_g$, where r is the radius of the AFT and D_g is the gas-phase diffusion coefficient of HO_2 (~0.25 cm^2 s^{-1}),[9] and this time is estimated to be ~7 s.[14] Furthermore, potential turbulent mixing of flows containing aerosol and radical might occur with a magnitude similar to that of gas-phase diffusion.[10] Therefore, we assumed that they are well mixed at ~4 s. In this study, the injection position of HO_2 radical was changed between 30 and 70 cm from the bottom of the AFT.

2.5. Aerosol Detection. A scanning mobility particle sizing (SMPS) instrument was used to observe aerosol distributions and concentrations. The SMPS instrumentation consisted of a differential mobility analyzer (DMA3080, TSI) for size selection followed by a condensation particle counter (CPC3010, TSI). Figure 2 shows a typical size distribution of NaCl wet aerosol at RH 53%. By scanning over the mobility diameter range of 10−420 nm, the distribution of aerosol number density (#), surface area density (S), and volume density (V) were determined. The aerosol concentrations of NaCl and $(NH_4)_2SO_4$ in this study were from 0.5×10^5 to 1.3×10^6 particles cm^{-3} for the number density, and the geometric standard deviation was 1.85 ± 0.05. If the aerosol distribution is well characterized by a log-normal radius distribution, the mean-surface-area-weighted radius r_s[14,15] can be determined by

$$r_s = r_{peak} \exp[2.5(\ln \sigma)^2] \quad (3)$$

where r_{peak} is the radius for the peak of the distribution and σ is the geometric standard deviation. In this study, $r_s = 80-110$ nm for wet particles, and $r_s = \sim 70$ nm for dry particles.

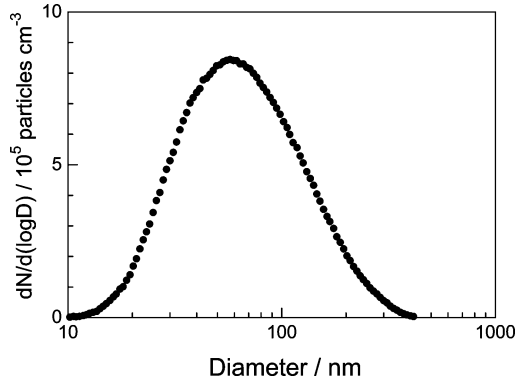

Figure 2. Number-weighted size distribution of wet (●) particles of NaCl at RH 53% using SMPS. The measured total number and surface area concentrations are 6.2×10^5 particles cm^{-3} and 1.73×10^{-4} cm^2 cm^{-3}.

The aerosol concentration after passing the AFT was ~10% lower than that before. The decrease is explained by the dilution by the flow containing radicals. Therefore, we concluded that the wall loss of aerosol was negligible.

2.6. Measurement of HO_2. The HO_2 was detected by CC/LIF-FAGE (fluorescence assay by gas expansion) technique. Details of the apparatus have been given in the previous studies.[16,17] Therefore, only a brief description important for this study is given here. The LIF instruments for measuring OH radicals can be applied for the selective measurement of HO_2 by chemical conversion just before the detection zone via the reaction of $HO_2 + NO \rightarrow OH + NO_2$. The transition line employed for excitation was the $Q_1(2)$ line of OH ($A^2\Sigma - X^2\Pi$, $v' = 0 - v'' = 0$). An excitation laser was operated at a repetition rate of 8 kHz. The LIF cell was evacuated continuously by a booster pump (PMB003CM, ULVAC) and a rotary pump (VD401, ULVAC). The total pressure in the LIF cell was about 2.3 Torr, which was measured by a capacitance manometer (Baratron 127, MKS). The LIF signals were detected by a channel photomultiplier (CPM, C1982P, Perkin-Elmer Optoelectronics) coupled with the photon-counting method through four lenses and a band-pass filter centered at 308 nm. The detection axis was perpendicular to both the gas flow and the laser excitation. A signal integration time of 5 min was adapted to achieve a low detection limit. The typical detection limit (S/N = 2, t = 60 s) of our instrument was 2×10^5 molecules cm^{-3}. By calibrating the instrument by the simultaneous photolysis of O_2 and H_2O,[16] the concentration of HO_2 radical in this study was estimated to be $\sim 3 \times 10^7$ and $\sim 1 \times 10^8$ molecules cm^{-3} at an injector position of 30 cm in the presence and absence of aerosols, respectively. This difference may be attributed to the uptake of HO_2 that occurs during mixing between HO_2 and aerosol particles.

In the HO_2 generator, OH radical is also generated by photolysis of H_2O (reaction 1). However, the OH signal measured without the addition of NO was always negligible. It is implied that OH radical generated by the photolysis of H_2O is lost by the wall and chemical reaction with trace amounts of impurity of zero air before reaching the bottom of the radical injection tube. Mie scattering caused by the aerosols did not significantly increase the background noise level in the LIF detection cell.

3. Results and Discussion

3.1. Data Analysis. Figure 3 shows injector-position-dependent profiles of HO_2 in the absence and presence of aerosol particles. The vertical axis in Figure 3 is in log scale, and the

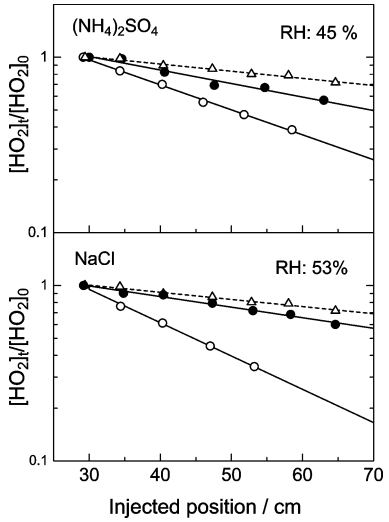

Figure 3. Injector position dependence of HO_2 signals at atmospheric pressure. Signal intensities are normalized to those at the initial injected position. The △ symbols indicate the background loss of HO_2. The ○ and ● symbols correspond to the wet and dry particles, respectively. The upper panel shows profiles of HO_2 in the presence of $(NH_4)_2SO_4$ aerosol particles. The total surface concentrations for dry and wet particles were 1.27×10^{-4} and 1.35×10^{-4} cm^2 cm^{-3}, respectively, at RH 45%. The lower panel shows profiles of HO_2 in the presence of NaCl aerosol particles. The total surface concentrations for dry and wet particles were 1.73×10^{-4} and 1.76×10^{-4} cm^2 cm^{-3}, respectively, at RH 53%. The fitting line is an exponential decay fit to the HO_2 injector position.

HO_2 signal intensity is normalized by that at the initial injected position. In this study, HO_2 decays were found to be exponential and are explained by first-order kinetics:

$$\frac{[HO_2]_t}{[HO_2]_0} = \exp(-k_{obs}t) \tag{4}$$

where $[HO_2]_0$ is the initial concentration of HO_2 radicals at the injector position, t is the reaction time, and k_{obs} is the effective first-order rate constant (s^{-1}) for heterogeneous reaction of HO_2 with the aerosol particles. The plot of $\ln([HO_2]_t/[HO_2]_0)$ as a function of t derived from the radical injected position and the flow velocity in the AFT gives k_{obs} as a slope of the straight line in the presence of aerosol. To exclude the HO_2 loss by the wall of the AFT from the observed decay, decay rates of HO_2 were measured at the same RH under the absence of aerosols for each experiment. The k_{obs} was employed to calculate uptake coefficient, γ_{obs}, after correction of wall loss and diffusion under non-plug conditions using techniques of Brown.[18] The corrected k_{obs} values were 10−20% higher than original values, where the measured wall loss rate was simply subtracted from the observed HO_2 decay.

The first-order rate constant (k_{obs}) is related to the observed uptake coefficient by

$$k_{obs} = \frac{\gamma_{obs}\omega_{HO_2}}{4}S \tag{5}$$

where ω_{HO_2} is the molecular thermal speed of HO_2 (cm s^{-1}), and S is the total surface concentration of aerosols (cm^2 cm^{-3}). In Figure 4, the observed first-order rate constants for HO_2 are plotted against the total surface concentrations of aerosol. The observed uptake coefficient (γ_{obs}) can be determined by slopes in Figure 4 using eq 5.

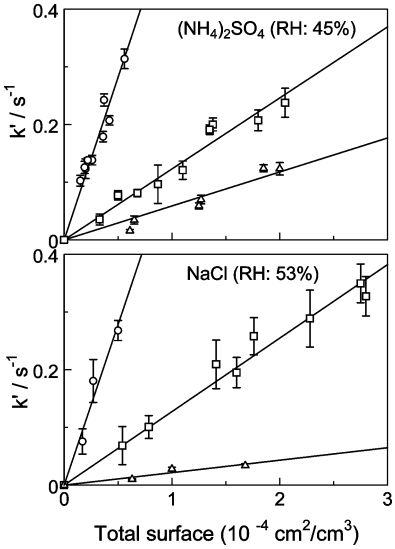

Figure 4. Plots of first-order decay rates (k') for HO_2 versus total surface concentration of aerosol particles. Upper and lower panels show results for $(NH_4)_2SO_4$ and NaCl, respectively. ○, □, and △ indicate wet particles doped with $CuSO_4$, wet particles, and dry particles, respectively.

However, in deriving γ_{obs} from eq 5, the gas-phase diffusion has not been taken into account. The coefficient γ_{obs} is modified to a corrected uptake coefficient γ_{corr} using the equations below.[19,20]

$$\gamma_{corr} = \frac{\gamma_{obs}}{(1 - \gamma_{obs}\lambda(r_s))} \tag{6}$$

Values of $\lambda(r_s)$ are given by

$$\lambda(r_s) = \frac{0.75 + 0.283K_n}{K_n(1 + K_n)} \tag{7}$$

where K_n is the Knudsen number defined by

$$K_n = \frac{3D_g}{\omega_{HO_2}r_s} \tag{8}$$

In the present study, $\lambda(r_s)$ was in a range from 0.15 to 0.25. The correction in this study was small, only 3% and 10% in the case of $\gamma_{obs} = 0.1$ and 0.5, respectively, for $r_s \approx 110$ nm. Hereafter, the corrected γ_{corr} is simply denoted as γ. The values of γ obtained in this study are listed in Table 1, together with the values reported previously. Quoted errors are two standard deviations from the least-squares fits, combined with the estimated systematic uncertainties in the measurements of aerosol surface concentration (5%) and flow speed (2%).

3.2. HO_2 Loss by Dry Aerosol Particles of $(NH_4)_2SO_4$ and NaCl. The γ values for dry particles of NaCl measured in this study were <0.01 and 0.02 ± 0.01 at RH 20% and 53%, respectively. The γ values for solid NaCl in the previous study at room temperature and under a low-pressure condition were 0.012 ± 0.002[7] and 0.016 ± 0.003,[8] which were in good agreement with our results. The γ values for dry particles of $(NH_4)_2SO_4$ in this study were 0.04 ± 0.02 and 0.05 ± 0.02 at RH 20% and 45%, respectively. For solid $(NH_4)_2SO_4$, the uptake coefficient has been reported to be 0.011.[8] For dry aerosol particles, the γ values are in general agreement with those from previous studies.

TABLE 1: Summary of Uptake Coefficient of HO_2 for Various Phases of NaCl and $(NH_4)_4SO_4$

NaCl	RH[a]	γ	methods[b]	refs
dry particles	20%	<0.01	ATF/CC/LIF	this work
	53%	0.02 ± 0.01	ATF/CC/LIF	this work
solid film		0.012 ± 0.001	ESR or EPR	7
		0.016 ± 0.003	EPR	8
wet particles	53%	0.11 ± 0.03	ATF/CC/LIF	this work
	63%	0.09 ± 0.02	ATF/CC/LIF	this work
	75%	0.10 ± 0.02	ATF/CC/LIF	this work
doped with $CuSO_4$	53%	0.65 ± 0.17	ATF/CC/LIF	this work

$(NH_4)_2SO_4$	RH[a]	γ	methods[b]	refs
dry particles	20%	0.04 ± 0.02	ATF/CC/LIF	this work
	45%	0.05 ± 0.02	ATF/CC/LIF	this work
solid film		0.011	EPR	8
wet particles	45%	0.11 ± 0.03	ATF/CC/LIF	this work
	42%	~0.1[c]	AFT/CIMS	10
	55%	0.15 ± 0.03	ATF/CC/LIF	this work
	65%	0.17 ± 0.04	ATF/CC/LIF	this work
	75%	0.19 ± 0.04	ATF/CC/LIF	this work
doped with $CuSO_4$	45%	0.53 ± 0.13	ATF/CC/LIF	this work
	42%	0.5 ± 0.1	AFT/CIMS	10

[a] Temperature is 296 K. [b] ATF/CC/LIF, aerosol flow tube coupled with a chemical conversion/laser-induced fluorescence technique; EPR, electron paramagnetic resonance; ESR, electron spin resonance; AFT/CIMS, aerosol flow tube coupled to a chemical ionization mass spectrometer. [c] The γ is given by the first-order analysis of the observed HO_2 decay.

3.3. HO_2 Loss by Wet Aerosol Particles Doped with $CuSO_4$. The γ values for wet particles of $(NH_4)_2SO_4$ and NaCl doped with $CuSO_4$ were 0.53 ± 0.12 and 0.65 ± 0.17, respectively. Previous reports[9,10] suggested that Cu(II) ions act as a scavenger for the catalytic reaction of HO_2 in the aqueous phase. Because the HO_2 radical undergoes acid dissociation ($HO_2(aq) \leftrightarrow H^+ + O_2^-$) in the aqueous phase, there are two loss processes ((9) and (11)) to initiate catalytic consumption of HO_2.

$$Cu^{2+} + HO_2(aq) \longrightarrow O_2(aq) + Cu^+ + H^+ \quad (9)$$

$$Cu^+ + HO_2(aq) \xrightarrow{H_2O} H_2O_2(aq) + Cu^{2+} + OH^- \quad (10)$$

$$Cu^{2+} + O_2^-(aq) \longrightarrow O_2(aq) + Cu^+ \quad (11)$$

$$Cu^+ + O_2^-(aq) \xrightarrow{2H_2O} H_2O_2(aq) + Cu^{2+} + 2OH^- \quad (12)$$

Rate constants for eqs 9−12 are 1.2×10^9, 1.5×10^9, 9.4×10^9, and 8.0×10^9 M^{-1} s^{-1}, respectively.[21−23] In the case of the wet aerosol particles generated at 45−55% RH, the molarity of Cu(II) is estimated to be ~0.5 M in the wet particles.[13] Thus, the lifetime of HO_2 is estimated to be less than 1 ns. The mass accommodation of gas HO_2 to the surface will be a rate-limiting step by scavenging in the aerosol particle by reaction with Cu^{2+}. Consequently, it is reasonable to conclude that the measured γ is equal to the mass accommodation coefficient (α).

There are only a few studies for the measurement of mass accommodation of HO_2 by wet particles at room temperature.[9,10] Their results gave 0.5 ± 0.1, 0.40 ± 0.08, and 0.94 ± 0.20 for the α of $(NH_4)_2SO_4$, $(NH_4)HSO_4$, and $LiNO_3$, respectively. It should be noted that this is the first report of a mass accommodation coefficient for wet NaCl particles. The above values are in general agreement with our result. The previous studies[9,10] and this study suggest the mass accommodation coefficient for inorganic aerosol is commonly large, >0.40.

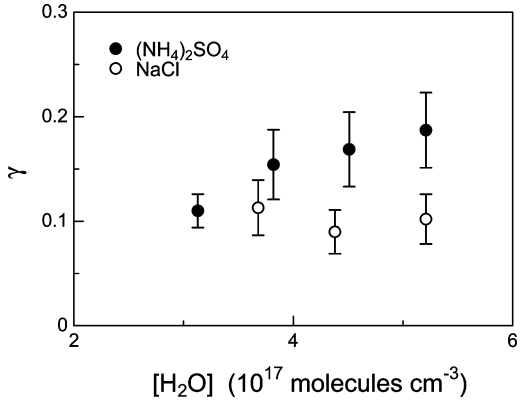

Figure 5. H_2O concentration dependence for uptake coefficients of HO_2 for wet aerosols of $(NH_4)_2SO_4$ (●) and NaCl (○).

3.4. HO_2 Loss by Wet Aerosol Particles. The γ values of $(NH_4)_2SO_4$ and NaCl were 0.11 ± 0.03 for 45% RH and 0.11 ± 0.03 for 53% RH, respectively. Figure 3 shows HO_2 profiles for the different phase aerosol particles of $(NH_4)_2SO_4$ and NaCl under almost identical total surface concentration and RH. The observed decay of HO_2 by both wet particles was larger than those by dry particles. This indicates that the uptake by wet particles was larger than that by dry particles under the same RH. This study was the first determination of γ for wet particles of NaCl. There was only one report with which to compare our result for wet $(NH_4)_2SO_4$ particles. Thornton and Abbatt[10] reported that γ for a wet aerosol of $(NH_4)_2SO_4$ buffered to pH = 5.1 was estimated to be ~0.1 from the first-order analysis of observed HO_2 decay at ~42% RH. This result is in good agreement with our result of 0.11 ± 0.03 at 45% RH. However, they reported that the observed HO_2 loss was attributed to self-reaction of HO_2 in the aqueous phase (eqs 13 and 14).

$$HO_{2(aq)} + HO_{2(aq)} \rightarrow H_2O_{2(aq)} + O_{2(aq)} \quad (13)$$

$$HO_{2(aq)} + O_2^-{}_{(aq)} + H_2O \rightarrow H_2O_{2(aq)} + O_{2(aq)} + OH^-{}_{(aq)} \quad (14)$$

Because the HO_2 concentration in their experiment was quite high (~5×10^{10} molecules cm^{-3}), assuming the surface concentration of HO_2 on a particle is in equilibrium with the bulk concentration, they reported the rate constants from observed HO_2 loss was in agreement with those from the literature, which were 8.6×10^5 and 1.0×10^8 M^{-1} s^{-1} for eqs 13 and 14, respectively.[24] Therefore, they concluded that the loss rate of HO_2 can be calculated on the basis of the known aqueous phase chemistry of eqs 13 and 14. When the HO_2 radical concentration becomes of the same order in the troposphere (~1×10^8 molecules cm^{-3}), the γ for wet particles of $(NH_4)_2SO_4$ will be less than 0.01 at ~42% RH from extrapolation. This result was inconsistent with our result of 0.11 ± 0.03 under [HO_2] ~1×10^8 molecules cm^{-3}. The reason for the inconsistency is unclear.

The γ values of $(NH_4)_2SO_4$ were 0.15 ± 0.03, 0.17 ± 0.04, and 0.19 ± 0.04 for 55%, 65%, and 75% RH, respectively. On the other hand, the γ values of NaCl were 0.09 ± 0.02 and 0.10 ± 0.02 for 63% and 75% of RH, respectively. Uptake coefficients determined in this study for wet particles of $(NH_4)_2SO_4$ and NaCl as a function of H_2O concentration (RH) are shown in Figure 5. An increasing trend with H_2O concentration is observed for wet $(NH_4)_2SO_4$ aerosol particles, while the γ values by NaCl were almost constant.

TABLE 2: Calculated Values of k_r and l for Wet $(NH_4)_2SO_4$ Aerosol Particles

RH (%)	r_s[a] (nm)	V/S[b] (10^{-6} cm)	k_r[c] (10^3 s^{-1})	l[d] (nm)
45	90	2.5	5.0	460
55	102	2.6	6.9	390
65	106	2.7	7.9	360
75	110	2.9	8.6	360

[a] r_s is determined from eq 3 using SMPS measurement. [b] V/S is a ratio of the total aerosol volume and surface. [c] k_r is calculated by eq 16. [d] l is the reacto-diffusive length calculated by $l = \sqrt{D_l/k_r}$ using the results from eq 16.

In the steady-state concentration of the HO_2 between a particle surface and just inside the surface, the measured γ for the reaction on the aerosol particle is given by Hanson at al.[25]

$$\frac{1}{\gamma} = \frac{1}{\alpha} + \frac{\omega}{4HRT\sqrt{D_l k_r}}\left(\coth q - \frac{1}{q}\right)^{-1} \qquad (15)$$

where H is the effective Henry's law constant, R is the gas constant, T is temperature, and D_l is the aqueous phase diffusion coefficient, assumed to be 10^{-5} cm^2 s^{-1} for HO_2.[22] k_r is the first-order rate constant for the reaction of HO_2 in the bulk aqueous phase, and q is the reacto-diffusive parameter, which is the ratio of particle radius r_s to the reacto-diffusive length l. This length (l) is a measure of the distance from the interface in which the reaction occurs, defined as $l = \sqrt{D_l/k_r}$.[25] This length may suggest reaction regimes, volume-limited reaction regime, and surface reaction regime, in the case of $l \gg r_s$ and $r_s \gg l$, respectively. When $r_s \gg l$, the factor $(\coth q - 1/q)^{-1}$ will become $\sim$1, and the uptake coefficient should not be dependent on particle size. When $l \gg r_s$, the reaction in the aqueous phase occurs throughout the entire particle volume. One possible explanation for the apparent RH dependence may lie in the potential effect of particle size due to the increasing water content with RH. In this case, γ becomes size-dependent and is given by

$$\frac{1}{\gamma} = \frac{1}{\alpha} + \frac{\omega}{4HRT(V/S)k_r} \qquad (16)$$

where V/S is a ratio of volume and surface of the total observed aerosol particles. Estimated values of k_r in eq 16 are listed in Table 2 together with corresponding l. The effective Henry's law constant (H_{eff}) was estimated by the equation $H_{eff} = H_{HO_2}(1 + K_{eq}^{HO_2}/[H^+])$. H_{HO_2} is Henry's law constant, and $K_{eq}^{HO_2}$ is the acid dissociation constant of HO_2 ($HO_{2(aq)} \leftrightarrow H^+_{(aq)} + O_2^-{}_{(aq)}$). H_{HO_2} and $K_{eq}^{HO_2}$ were 4000 (M atm^{-1})[24] and 2.1×10^{-5} (M),[22] respectively, and $[H^+]$ that was estimated by the concentration in the particles was $\sim 10^{-4.2}$ (M) in the range of 45−75% RH. T, D_l, and ω have already been mentioned above, and α was 0.53 as determined in this study. Estimated values of k_r increased with RH, and the values of l were $\sim$500 nm. k_r and l were also estimated using eq 15. The values of k_r were 20% less than those from eq 16, and l had values similar to those from eq 16. These results suggest that the reaction may lie in the transition region between volume- and surface-dependent processes, because l is of the same order as r_s. Overall, the estimated l values were about 4 times larger than r_s. This implies that the uptake is not fully volume-limited, but may be a mostly volume-limited process. The k_r value still increased with RH (Table 2), suggesting that the dependence of γ for wet $(NH_4)_2SO_4$ particles on RH cannot be explained only by the changes in the Henry's law constant and in the V/S ratio associated by the increasing water content with RH. Apparently, the dependence of k_r on RH needs to be explained by chemical reactions. In this system, reactants should be H_2O. The concentration of H_2O in the particle will increase due to an increasing water content with RH, while the concentration of ions (NH_4^+ and SO_4^{2-}) in particles will decrease with RH. If the reactions of HO_2 in the particles with the NH_4^+ or SO_4^{2-} have significant contribution loss of HO_2, the HO_2 loss should decrease due to a decreasing ion concentration with RH. Therefore, the reactivity of H_2O in a particle for HO_2 loss may be more significant than that of ions in the case of $(NH_4)_2SO_4$. On the other hand, in the case of a wet NaCl aerosol particle, there was no tendency of γ on RH. Although we cannot suggest that reaction scheme for loss of HO_2 in the particles, one possible explanation is that the presence of H_2O and ions (Cl^- or Na^+) in the particle is significant for HO_2 loss. As a result, both contributions to HO_2 loss might be canceled by increasing water content and decreasing ion concentrations with RH. The ions present in the wet $(NH_4)_2SO_4$ particle might be less reactive than Cl^- or Na^+. However, there are no data to verify these hypotheses. More information is needed for HO_2 chemistry in aqueous phase. The measurements of the uptake coefficient of HO_2 by $(NH_4)HSO_4$, H_2SO_4, and KCl particles are planned. These results would give more systematic information to argue the loss mechanism of HO_2 in the wet particles including the key ions, NH_4^+, SO_4^{2-}, Na^+, and Cl^-.

Under humid conditions, HO_2 radical in the gas phase can generate water-complexed HO_2, $HO_2{-}H_2O$.[26] The equilibrium for $HO_2 + H_2O \leftrightarrow HO_2{-}H_2O$ was established quickly, and the constant (K_{eq}) was reported as $(5.2 \pm 3.2) \times 10^{-19}$ $molecule^{-1}$ cm^3.[27,28] Under a relative humidity of 45%, 55%, 65%, and 75%, the ratio of $[HO_2{-}H_2O]/[HO_2]$ will be 0.16, 0.20, 0.23, and 0.27, respectively. Another possible explanation of the apparent RH dependence for γ by wet $(NH_4)_2SO_4$ particles is the contribution of the $HO_2{-}H_2O$ complex. The uptake coefficients of HO_2 and $HO_2{-}H_2O$ to the wet particle could be different. Aloisio et al.[29] suggested there is a possibility of $HO_2{-}H_2O$ loss by the aerosols.

$$HO_2{-}H_2O + \text{aerosol} \rightarrow \text{products} \qquad (17)$$

However, they did not study the process further. It is likely that our detection technique does not detect the $HO_2{-}H_2O$. If the increase in the loss of observed HO_2 with RH was fully attributable to the consumption of $HO_2{-}H_2O$ by aerosols, we should modify the previous analysis. Here, when the equilibrium between HO_2 and HO_2H_2O is established, the uptakes of $HO_2{-}H_2O$ and HO_2 by $(NH_4)_2SO_4$ aerosols were simply calculated by

$$k_{obs} = k'_{HO_2} + k'_{HO_2-H_2O} \qquad (18)$$

$$k_{obs} = \gamma'_{HO_2}\frac{\omega_{HO_2}}{4}S + \gamma'_{HO_2-H_2O}\frac{\omega_{HO_2-H_2O}}{4}SK_{eq}[H_2O] \qquad (19)$$

where $\omega_{HO_2-H_2O}$ is the molecular thermal speed of $HO_2{-}H_2O$, and γ'_{HO_2} and $\gamma'_{HO_2-H_2O}$ were estimated to be 0.02 and 0.88, respectively, to fit the dependence of k_{obs} on $[H_2O]$. In this assumption, overall uptake coefficients ($\gamma_{overall}$) by wet $(NH_4)_2SO_4$ aerosols, which were calculated for averaged molecular thermal speed for $HO_2{-}H_2O$ and HO_2, were 0.12, 0.16, 0.18, and 0.20 for 45%, 55%, 65%, and 75% RH, respectively. Taking account of the contribution of $HO_2{-}H_2O$, $\gamma_{overall}$ will be $\sim$10% larger than γ.

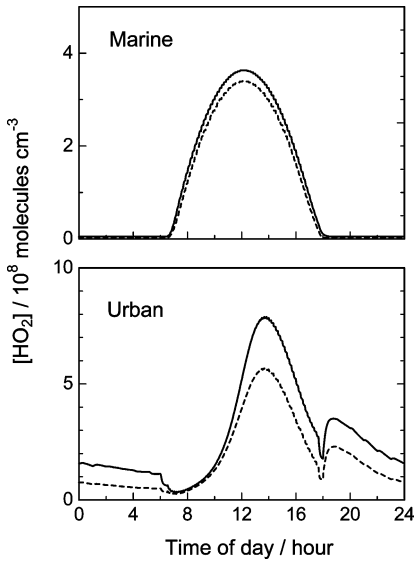

Figure 6. Diurnal variations of the HO_2 concentration calculated with $\gamma = 0$ (solid line). Broken lines indicate the HO_2 concentration calculated with $\gamma = 0.1$ and 0.15 for marine and urban cases, respectively.

4. Atmospheric Implications

Our results suggest that the uptake coefficient of HO_2 by aerosols depends on phase, composition, and RH. The γ values by solid aerosol (NaCl and $(NH_4)_2SO_4$) were <0.05, while they were enhanced to 0.09−0.19 once the particles became wet. In our results, we recommend that the uptake coefficient of HO_2 by wet particles of NaCl is 0.10 with no dependence on RH. Because those by wet particles of $(NH_4)_2SO_4$ depend on RH, we tentatively suggest an averaged value of $\gamma_{((NH_4)_2SO_4)} = 0.15$.

To estimate the contribution of the heterogeneous loss for HO_2, we carried out the box model calculation for the diurnal variation of HO_2 concentration for the remote marine and the urban cases. We adapted $\gamma_{NaCl} = 0.10$ and $\gamma_{(NH_4)_2SO_4} = 0.15$ to the remote marine and the urban cases, respectively, and the gas-phase diffusion coefficient of HO_2 ($\sim$0.25 cm^2 s^{-1}). The other parameters for the box model calculation were the same as those in ref 11. Under the typical aerosol concentration, the first-order decay rates of heterogeneous loss for the remote marine and urban cases were estimated to be 9.6×10^{-4} and 1.8×10^{-2} s^{-1}, respectively. Figure 6 shows diurnal variations of HO_2 with and without heterogeneous loss. The concentrations of the daytime maximum of HO_2 without heterogeneous loss were 3.6×10^8 and 7.9×10^8 molecules cm^{-3} for marine and urban cases, respectively. With heterogeneous loss, the HO_2 concentrations became 3.4×10^8 and 5.6×10^8 molecules cm^{-3} for the marine and urban cases, respectively. It was clear that the contribution of the heterogeneous loss in the HO_2 variation is significant.

Martin et al.[12] reported the contribution of heterogeneous loss of HO_2 in the HO_x loss with an assumption of $\gamma = 0.2$ by global tropospheric modeling. In their modeling, the sea salt and sulfate aerosols contributed heterogeneous HO_2 loss in the Antarctic region and Northern Hemisphere. The loss of HO_2 will be overestimated in these regions, because the uptake coefficient by wet particles was less than 0.2 from our results.

If the aerosol contains Cu^{2+} ions, γ increases due to the acceleration of HO_2 loss by the chemical reaction in the particle. Although the rate constant for $Fe^{2+} + HO_2$ is a few orders smaller than that for $Cu^{2+} + HO_2$,[23] Fe^{2+} ions may also be significant for HO_2 loss. This is because Fe and Cu are ubiquitous and the concentration of Fe is larger than that of Cu. Concentrations in the rural area are reported to be in the range 0.06−15 and 0.003−0.3 μg m^{-3} for Fe and Cu, respectively.[30] Consequently, wet particles have a potentially high contribution of the heterogeneous reaction, while there is a possibility that these metals are not fully free ions in the aqueous phase.[23] An understanding of the composition and surface condition in the aerosol particles is important for an estimation of the heterogeneous effect.

5. Summary

We reported the HO_2 uptake coefficient for submicron wet and dry aerosols ($(NH_4)_2SO_4$ and NaCl) under atmospheric pressure at 296 ± 2 K using an aerosol flow tube coupled with a chemical conversion/laser-induced fluorescence (CC/LIF) technique. This study was carried out under HO_2 concentrations of $\sim 1 \times 10^8$ molecules cm^{-3}, which were similar to the ambient concentration levels. The uptake coefficients of dry aerosol (NaCl and $(NH_4)_2SO_4$) particles were <0.05. On the other hand, the uptake coefficients of wet particles of NaCl and $(NH_4)_2SO_4$ were estimated to be 0.10 and 0.15, respectively, which suggested that heterogeneous loss was enhanced by the particle containing water. Furthermore, the γ value for wet $(NH_4)_2SO_4$ particles depended on RH. We discussed the potential loss mechanisms for HO_2. One possible mechanism was a particle size-limited process, in which H_2O in the particle is significant for HO_2 loss. Another possibility was attributed to HO_2–H_2O loss by aerosols. However, we cannot identify the loss mechanism of HO_2 radical shown above. More data are needed to understand the heterogeneous loss mechanism of HO_2. Finally, to estimate the contribution of heterogeneous loss of HO_2 by aerosol, the diurnal variation of HO_2 using a box-model calculation was demonstrated. As a result, the daytime maximum concentrations of HO_2 were changed to 95% and 70%, relative to an absence of heterogeneous loss for marine and urban areas, respectively.

Acknowledgment. This research has been supported by the Global Environmental Research Fund (B-051), the Japan Ministry of Environment, and a Grant-in-Aid for Scientific Research (KAKENHI) (C) 19510026.

References and Notes

(1) Finlayson-Pitts, B. J.; Pitts, J. N., Jr. *Chemistry of the Upper and Lower Atmosphere, Theory, Experiments, and Applications*; Academic Press: New York, 2000.

(2) Carslaw, N.; Creasey, D. J.; Heard, D. E.; Jacobs, P. J.; Lee, J. D.; Lewis, A. C.; McQuaid, J. B.; Pilling, M. J.; Bauguitte, S.; Penkett, S. A.; Monks, P. S.; Salisbury, G. *J. Geophys. Res.* **2002**, *107*, doi: 10.1029/2001JD001568.

(3) Sommariva, R.; Haggerstone, A.-L.; Carpenter, L. J.; Carslaw, N.; Creasey, D. J.; Heard, D. E.; Lee, J. D.; Lewis, A. C.; Pilling, M. J.; Zádor, J. *Atmos. Chem. Phys.* **2004**, *4*, 839−856.

(4) Kanaya, Y.; Sadanaga, Y.; Matsumoto, J.; Sharma, U. K.; Hirokawa, J.; Kajii, Y.; Akimoto, H. *J. Geophys. Res.* **2000**, *105*, 24205.

(5) Kanaya, Y.; Cao, R.; Kato, S.; Miyakawa, Y.; Kajii, Y; Tanimoto, H.; Yokouchi, Y.; Mochida, M.; Kawamura, K.; Akimoto, H. *J. Geophys. Res.* **2007**, *112*, D11308, doi: 10.1029/2006JD007987.

(6) Creasey, D. J.; HalfordMaw, P. A.; Heard, D. E.; Pilling, M. J.; Whitaker, B. J. *J. Chem. Soc., Faraday Trans.* **1997**, *93*, 2907.

(7) Remorov, R. G.; Gershenzon, Y. M.; Molina, L. T.; Molina, M. J. *J. Phys. Chem. A* **2002**, *106*, 4558.

(8) Gershenzon, Y. M.; Grigorieva, V.; Ivanov, A. V.; Remorov, R. G. *Faraday Discuss.* **1995**, *100*, 83.

(9) Mozurkewich, M.; McMurry, P. H.; Gupta, A.; Calvert, J. G. *J. Geophys. Res.* **1987**, *92*, 4163−4170.

(10) Thornton, J.; Abbatt, J. P. D. *J. Geophys. Res.* **2005**, *110*, D08309, doi: 10.1029/2004JD005402.

(11) Morita, A.; Kanaya, Y.; Francisco, J. S. *J. Geophys. Res.* **2004**, *109*, D09201, doi: 10.1029/2003JD004240.

(12) Martin, R. V.; Jacob, D. J.; Yantosca, R. M.; Chin, M.; Ginoux, P. *J. Geophys. Res.* **2002**, *108*, 4097.
(13) Martin, S. T. *Chem. Rev.* **2000**, *100*, 3403.
(14) Hanson, D.; Kosciuch, E. *J. Phys. Chem. A* **2003**, *107*, 2199.
(15) Lovejoy, E. R.; Huey, L. G.; Hanson, D. R. *J. Geophys. Res.* **1995**, *100*, 18, 775.
(16) Kanaya, Y.; Akimoto, H. *Appl. Opt.* **2006**, *45*, 1254.
(17) Kanaya, Y.; Sadanaga, Y.; Hirokawa, J.; Kajii, Y.; Akimoto, H. *J. Atmos. Chem.* **2001**, *38*, 73.
(18) Brown, R. L. *J. Res. Natl. Bur. Stand.* **1978**, *83*, 1.
(19) Fuchs, N. A.; Sutugin, A. G. *Highly Dispersed Aerosols*; Ann Arbor Sci.: Ann Arbor, MI, 1970.
(20) Fried, A.; Henry, B. E.; Calvert, J. G.; Mozurkewich, M. *J. Geophys. Res.* **1994**, *99*, 3517.
(21) Cabelli, D. E.; Bielski, B. H. J.; Holcman, J. *J. Am. Chem. Soc.* **1987**, *109*, 3665.
(22) von Piechowski, M.; Nauser, T.; Hoigne, J.; Buehler, R. E. *Ber. Bunsen-Ges. Phys. Chem.* **1993**, *97*, 762.
(23) Jacob, D. J. *Atmos. Environ.* **2000**, *34*, 2131.
(24) Bielski, B. H. J. *Photochem. Photobiol.* **1978**, *25*, 645.
(25) Hanson, D. R.; Burkholder, J. B.; Howard, C. J.; Ravishankara, A. R. *J. Phys. Chem.* **1992**, *96*, 4979.
(26) Hamilton, E. J., Jr.; Lii, R.-R. *Int. J. Chem. Kinet.* **1977**, *9*, 875.
(27) Kanno, N.; Tonokura, K.; Tezaki, A.; Koshi, M. *J. Phys. Chem. A* **2005**, *109*, 3153.
(28) Kanno, N.; Tonokura, K.; Koshi, M. *J. Geophys. Res.* **2006**, *111*, D20312, doi: 10.1029/2005JD006805.
(29) Aloisio, S.; Francisco, J. S.; Friedl, R. R. *J. Phys. Chem. A* **2000**, *104*, 6597.
(30) Schroeder, W. H.; Dobson, M.; Kane, D. M.; Johnson, N. D. *JAPCA* **1987**, *37*, 1267.